ACI STRUCTURAL JOURNAL TECHNICAL PAPER

Title No. 113-S86

Cyclic Testing and Assessment of Columns Containing Recycled Concrete Debris

by F. Soleimani, M. McKay, C. S. W. Yang, K. E. Kurtis, R. DesRoches, and L. F. Kahn

Reuse of concrete debris as a component of structural concrete is important both economically and environmentally. In resource-poor regions, using construction debris may facilitate economic, rapid, material sourcing and debris disposal if it demonstrates adequate structural performance. To investigate the seismic resistance of structural elements with recycled concrete aggregate, this research performs quasi-static cyclic testing on four full-scale reinforced concrete columns—two containing natural aggregate and two containing recycled concrete aggregate—under both axial and lateral loads. For each aggregate source, reinforcement detailing in one column conformed to the seismic provisions in the International Building Code, while the detailing in the other column conformed to nonseismic design specifications. A pre-experimental numerical model for each column was created in OpenSees to predict the behavior of the column. Experimental and numerical results verify that seismically designed columns made of either natural aggregate concrete or recycled aggregate concrete show similar cyclic lateral behavior.

Keywords: columns; cyclic loading; recycled concrete aggregate; reinforced concrete; seismic performance.

INTRODUCTION

The Caribbean is a region with an unusually high exposure to both earthquakes and hurricanes. For example, the Jan. 12, 2010, 7.0-magnitude earthquake of Haiti damaged nearly half of the structures in the epi-central area and caused critical damage or even collapse to more than 300,000 homes and 30,000 businesses.[1] Damage to buildings and infrastructure due to earthquakes and hurricanes has resulted in a constant need for repair and reconstruction.

The Caribbean region is also resource-constrained.[2] Specifically, the availability of high-quality and economical sources of aggregates varies considerably among countries. Cement is produced in only a few locations in the Caribbean and must be shipped to other locations, while supplementary cementitious materials (SCMs), commonly used in much of the world's concrete, are seldom available.

Island nations are also space-constrained. As a result, the environmental impact of the disposal of large volumes of debris resulting from building collapses or subsequent demolition can be large. Together, these realities present significant challenges for reconstruction after natural disasters. The current research investigated the potential that debris material resulting from such an event or cascading events could be safely and economically reused in rebuilding efforts. Specifically, this research examines whether new concrete infrastructure produced with large amounts of debris material as recycled concrete aggregate (RCA) could support ordinary loading as well as exhibit resistance to subsequent natural hazards.

Extensive use of recycled concrete as aggregate dates to the period after World War II, when large quantities of concrete debris became available from damaged structures, as well as due to a sudden increase in demand for aggregate when damaged structures were to be reconstructed or repaired.[2] The productive reuse of recycled concrete as aggregate, rather than landfilling it, can potentially reduce the environmental impact associated with reconstruction. In particular, when the transit of the recycled material is less than the combined mileage for disposal of debris and the mileage traveled by natural aggregate for construction, recycling can be a sustainable option.

Research by Mwasha and Lalla[3] and Lalla and Mwasha[4] investigated the strength of concrete manufactured from recycled Guanapo coarse and fine aggregates sieved from construction and demolition waste (CDW), which were obtained from refuse concrete cylinders tested in compression in a laboratory. Concrete produced using CDW showed comparable properties to that of its source waste material and indicated a potential for reuse of CDW. However, in this study, only a limited range of properties (for example, compressive and splitting tensile strength) were measured.

While various research efforts have examined the influence of recycled concrete aggregate on concrete properties, mainly focusing on compressive strength, modulus, and workability,[3-5] relatively less research has examined the seismic behavior of concrete containing large volumes of recycled concrete as coarse aggregate. For example, to assess the applicability of recycled aggregate concrete (RAC) for structural elements, Corinaldesi et al.[6] investigated the behavior of beam-column joints by using concrete elements that were made of recycled concrete aggregates and natural aggregates, and that were subjected to cyclic loading. The recycled concrete aggregate was prepared by replacing 30% of coarse natural aggregates with recycled aggregates. Comparison of compressive, tensile, flexural, and bond strengths with reinforcing steel bars, as well as static elastic modulus, indicated that the performance of RAC and natural aggregate concrete (NAC) were similar. In particular, the assessment of cyclic loading test results such as cracking patterns, supplied and dissipated energy, and ductility indicated that the beam-column joint made of RAC showed adequate structural behavior.

ACI Structural Journal, V. 113, No. 5, September-October 2016.

MS No. S-2015-121.R3, doi: 10.14359/51689024, was received October 10, 2015, and reviewed under Institute publication policies.

Fig. 1—Recycled construction debris used as coarse aggregate (left) in concrete (right).

Table 1—Properties of concrete mixtures

Mixture	*w/c*	Cement, lb (kg)	Water, lb (kg)	Fine aggregate, lb (kg)	NCA, lb (kg)	RCA, lb (kg)
Control	0.53	550 (250)	292 (133)	1239 (562)	1767 (802)	—
RAC	0.53	550 (250)	292 (133)	1239 (562)	353 (160)	1524 (691)

*Values are corresponding to designed volume of 27 ft^3 (0.765 m^3) of concrete.

Although the effect of the reinforcement detailing of reinforced concrete (RC) columns with NAC has been investigated in several studies, the results have not been verified for the RC columns with RAC. Reviewing experimental results obtained during various shake-table tests for RC columns with natural aggregate, Elwood and Moehle[7] concluded that the lateral displacement (drift) of an RC column at axial failure is inversely proportional to the spacing of transverse reinforcement. Results from the research of Tasai[8] and Minowa et al.[9] on RC columns with natural aggregate indicated that the columns with closer transverse reinforcement spacing, which exhibited larger lateral displacement after shear failure, showed better performance than columns with widely spaced stirrups.

Although the numerical modeling of RC columns with natural aggregate has improved, structural models for RC frames do not consider the influence, if any, of recycled aggregate. Therefore, the applicability of the existing models needed to be evaluated for RC columns with RAC. Flores[10] used experimental column hysteretic data to calibrate the *OpenSees*[11] analytical model of shear-critical RC columns under gravity and seismic loading. The study was limited to RC columns with natural aggregates and characterized by a shear failure mode assuming that the RC column specimen behaved as a two-dimensional column under a cyclic, unidirectional lateral loading and constant gravity load. With appropriate calibration and further validation, a revised *OpenSees* program could be used to predict the hysteretic response of existing shear-critical RC beam-column frames under seismic and gravity loading.

The primary objective of the current research was to examine the viability of using large percentages of recycled coarse aggregates as a suitable substitute for natural aggregates, to investigate the cyclic behavior of columns with recycled concrete aggregate, and evaluate the accuracy of the RC column model in *OpenSees* for NAC and RAC. Four full-scale RC columns (two containing NAC and two containing RAC) were constructed and tested under cyclic loading conditions. For each aggregate type, reinforcement detailing in one column conformed to seismic provisions with Seismic Design Category D, E, or F in the *International Building Code* (IBC),[12] and the reinforcement in the other column was designed according to nonseismic provisions. The progression of damage was observed and recorded under the cyclic loading.

RESEARCH SIGNIFICANCE

From economic and environmental considerations, reusing concrete debris from natural disasters is important in relieving concerns regarding the disposal of concrete debris and the limited access to concrete aggregates for reconstruction. This study provides insight on the behavior of RC columns constructed using high volumes of recycled concrete coarse aggregates in comparison with columns constructed using natural aggregates. Results show that columns made with recycled concrete but designed in compliance with seismic provisions exhibit a very similar cyclic lateral response compared to the natural aggregate concrete columns, even though the compressive strength of recycled concrete was lower than that of natural aggregate concrete.

MATERIALS

The recycled concrete aggregate was obtained from a commercial concrete recycler in Florida, in a region where a relatively lower-strength Pleistocene limestone aggregate is common. This source of RCA is commonly used in nonstructural applications such as underlayment of concrete pipe. Also, while this coarse material is predominantly crushed concrete, some minor amounts of other construction debris (for example, ceramic tile, asphalt concrete, brick) were also present, as is evident in Fig. 1. This source was selected in an attempt to approximate the quality of the RCA that may be typical in the Caribbean region and also to encompass the variability that may be expected from construction debris more generally.

Two companion concrete mixtures were produced that differed in their source of aggregate. The first mixture contained natural aggregates ("Control" mixture), and the second mixture ("RAC" mixture) replaced natural coarse aggregate with recycled concrete aggregates (Fig. 1) at a rate of 81% by mass or 82% by volume, as shown in Table 1. The specific gravity (SG) of the RCA source was 2.44, and its absorption capacity was 12%. The natural coarse aggregate was crushed granitic gneiss (SG = 2.63) sourced from Lithonia, GA, with an absorption capacity of 0.4%. Both the RCA and the natural aggregate had a maximum size (MSA) of 1 in. (25.0 mm) and met gradation requirements for No. 57 stone in AASHTO M43.[13]

The concrete mixture used in this study was designed to achieve a 28-day compressive strength of 3500 psi (24.1 MPa). Test cylinders, 4 x 8 in. (101.6 x 203.2 mm), were cast from each mixture for compressive strength tests at different ages up to 28 days following procedures in ASTM C39.[14] Elastic modulus was measured on 6 x 12 in. (152.4 x 304.8 mm) at 28 days by ASTM C469.[15]

CYCLIC LOADING TESTS

Experimental approach

Four RC column specimens were constructed: two of the specimens (Specimens No. 1 and No. 2) were built using the NAC mixture (Control), and the other two (Specimens No. 3 and No. 4) were made with the RAC mixture. Figure 2 shows the results of concrete cylinder compression testing up to 28 days. The compressive strengths of natural concrete and recycled concrete were approximately 4500 and 2800 psi (31.0 and 19.3 MPa), respectively, and the elastic moduli were 3300 ksi (22,753 MPa) for NAC and 3820 ksi (26,338 MPa) for RAC (Table 2). Both mixtures were designed by ACI[16] methods to achieve similar strength values, and each contained the same amount of cement. The lower strength of RAC could be due to a variety of factors, including the lower intrinsic strength of RAC as well as its physical properties (for example, shape and surface texture), which may influence bond with the hydrated cement paste. Because the strength of the RAC concrete was close to the average strength (3000 psi [20.7 MPa]) of concrete produced in the Caribbean region,[17] it was deemed suitable for this evaluation.

While it has been conventionally reported that elastic modulus for RAC is typically lower than for NAC,[18,19] slightly greater (~15%) values were measured herein for the RAC. More recently, Rahal[5] has reported elastic moduli within 3% when comparing normal-strength (3625 to 4350 psi [25 to 30 MPa]) RAC and NAC. The values measured herein suggest that the elastic modulus with RAC need not necessarily be lower than that for NAC. It is proposed that in the case of lower- to normal-strength concrete, such as examined herein,

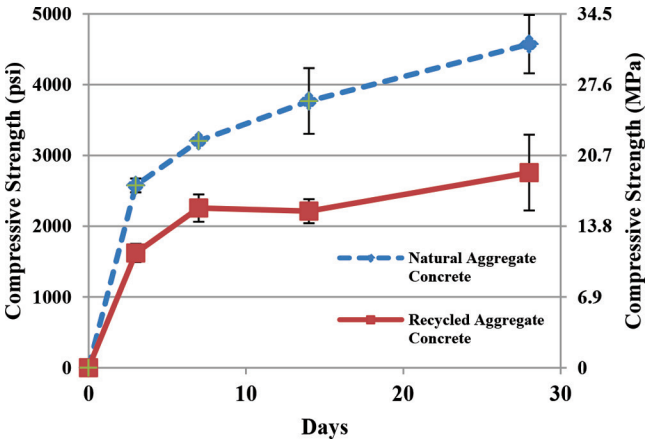

Fig. 2—Compressive strength development of concrete mixtures.

Table 2—Comparison of analytical and experimental results

Specimen	RC1	RC2	RC3	RC4
f_c', psi (MPa)	4500 (31.0)	4500 (31.0)	2800 (19.3)	2800 (19.3)
E_c, ksi (MPa)	3300 (22,753)	3300 (22,753)	3820 (26,338)	3820 (26,338)
$\Delta y_{(analytical)}$, in. (mm)	0.58 (14.7)	0.64 (16.3)	0.53 (13.5)	0.60 (15.2)
$\Delta y_{(experimental)}$, in. (mm)	0.40 (10.2)	0.63 (16.0)	0.30 (7.6)	0.47 (12.0)
Base shear ratio (be/bn) at 1% drift	0.89	0.81	0.97	0.91
Base shear ratio (be/bn) at 2% drift	0.97	0.93	1.13	1.23

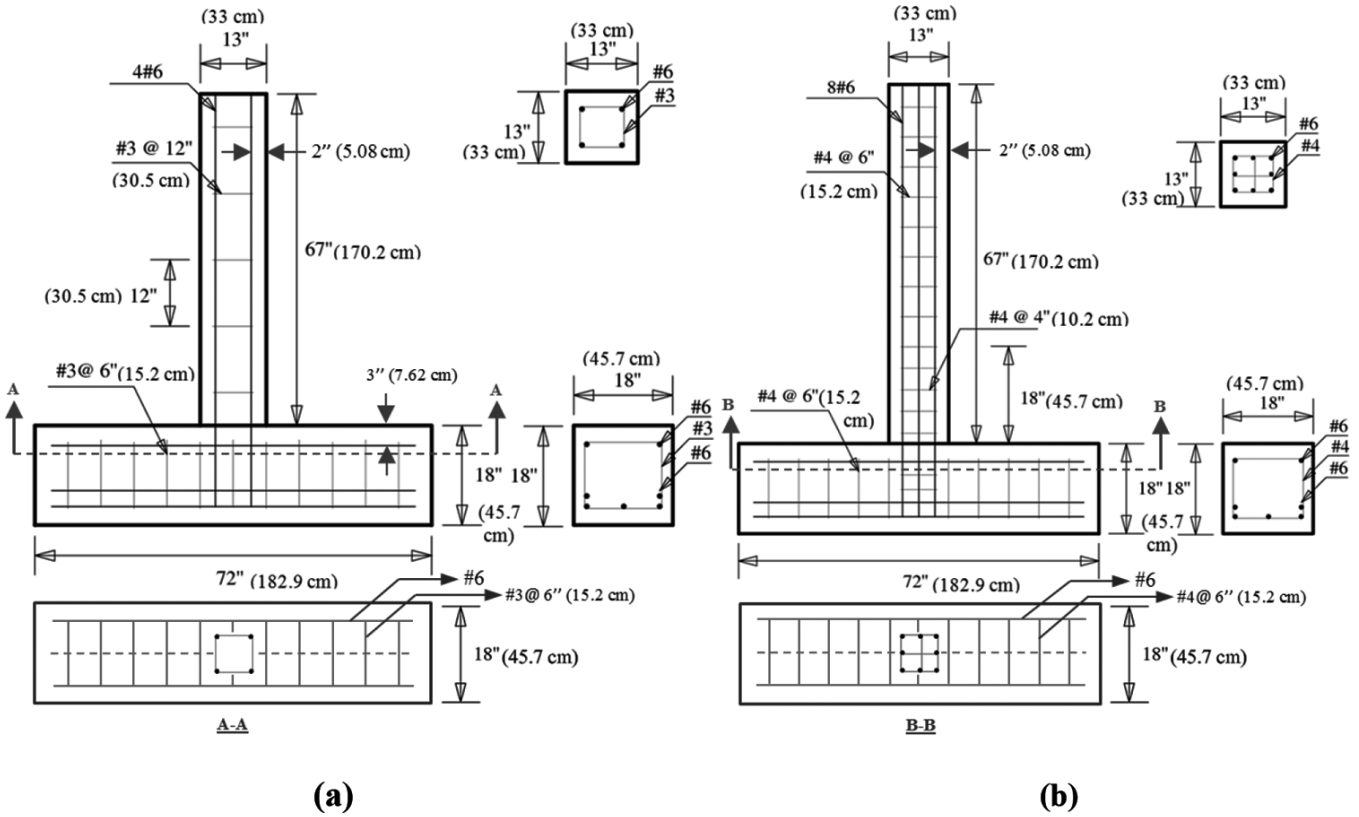

Fig. 3—Cantilever RC column specimens: (a) Specimens No. 1 and 3; and (b) Specimens No. 2 and 4.

similar elastic moduli may be found for comparable RAC and NAC. While further research will be needed to better understand the factors that influence this behavior, it is suggested that the higher absorption capacity of recycled concrete aggregate, which potentially increases bonding between the aggregate and paste diminishing transition zone effects, as well as greater elastic match between the RAC and the moderate strength paste, may play roles in improving the aggregate/paste bond.[20] Densification and reduced microcracking in the interfacial region are well-known to be correlated with increased modulus in concrete.[21,22]

Structural design of Specimens No. 2 and No. 4 conformed to IBC seismic provisions with Seismic Design Category D, E, or F. The other two specimens (Specimens No. 1 and No. 3) were structurally designed using nonseismic design standards, which have been used for fabricating nonductile columns found throughout the Caribbean. The longitudinal reinforcement in the columns was extended to the bottom of the foundation with a 90-degree hook at a clear cover of 3 in. (76.2 mm), as illustrated in Fig. 3.

The nonseismically designed columns were made using 1% reinforcement ratio with four No. 6 longitudinal bars and No. 3 ties spaced at 12 in. (304.8 mm) center-to-center (c/c). For the seismically designed columns, 2% reinforcement ratio was used, including eight No. 6 longitudinal bars and No. 4 ties spaced at 4 in. (101.6 mm) c/c at the bottom of the column to a height of 18 in. (457.2 mm) and then spaced at 6 in. (152.4 mm) c/c for the remainder of the column. The test specimens were cast in a flat, horizontal position. Steel reinforcement cages were built using Grade 60 steel for all column reinforcement. The details of the nonseismically and seismically designed columns are shown in Fig. 3(a) and 3(b), respectively.

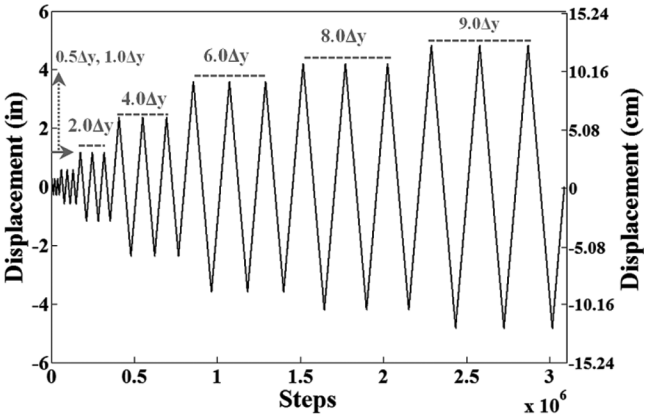

Fig. 4—Loading protocol applied to column Specimen No. 2.

Experimental setup

Quasi-static testing was selected to observe the sequence of damage in the RC column specimens under lateral and axial loading. A static axial load equal to 10% of the undamaged column calculated axial load capacity was applied to each specimen.[10,23] Reversed cyclic lateral loads were applied at the top of the columns, as illustrated in Fig. 4. The lateral loading cycles were sets of increasing amplitudes of lateral displacements[10]: 0.5Δy, 1.0Δy, 2.0Δy, 4.0Δy, 6.0Δy, 8.0Δy, and 9.0Δy (in which Δy refers to the calculated yield displacement), with three cycles at each level applied using a computer-controlled hydraulic actuator. The values of Δy obtained from analytical computations and experiments were in the range of 0.53 to 0.64 in. (13.5 to 16.3 mm) and of 0.30 to 0.64 in. (7.6 to 16.5 mm), respectively, as shown in Table 2.

Figure 5 illustrates the test setup. Axial loading was applied by posttensioning two vertical bars attached to a horizontal HSS section attached to the top of the column. The lateral load was applied with a horizontal actuator attached to a strong wall. Pin connections assured no flexural restraint from either loading apparatus. Quantitative measurements of strains in the columns were measured using electrical resistance strain gauges attached at various locations to the steel reinforcement (Fig. 6). The strain gauge measurements were used to calculate curvature of the columns.

Experimental results

Figure 7 presents visual observation of progressive damage to the specimens during the tests. Table 3 shows the degradation occurring in each test specimen based on the observed damage progression at each cycle drift ratio (the ratio of maximum lateral displacement to the height of the column).

Because the axial loading direction was always parallel to the column during the tests, rather than being purely vertical, the axial loading generated a horizontal force component

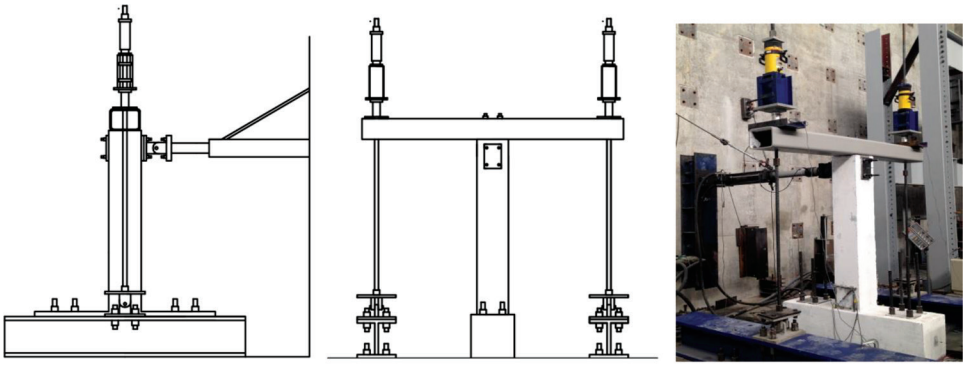

Fig. 5—(a) Schematic lateral view of experimental setup; (b) schematic lateral view of front view; and (c) lateral and axial loading systems.

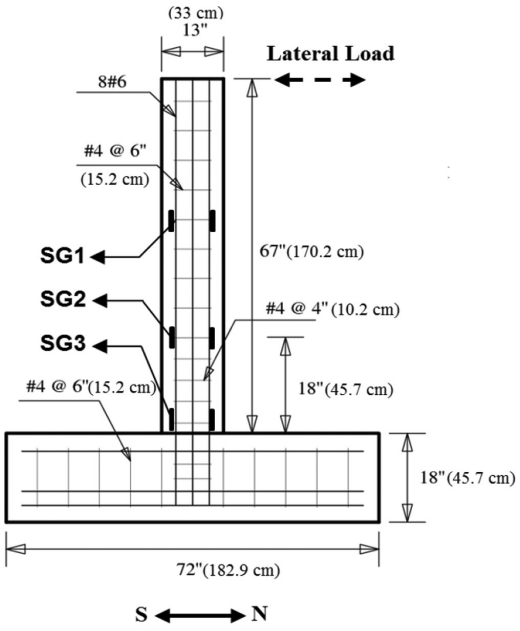

Fig. 6—(a) Location of strain gauges in experiments; and (b) recorded points of column section in numerical models.

upon the columns at all non-zero lateral displacements (Fig. 8). All specimens developed similar axial horizontal forces due to the same geometry of samples and similar axial loadings. The horizontal component of axial force had a magnitude of approximately 6 kip (26.7 kN) at maximum lateral displacement. Accordingly, the base shear in the columns was obtained by subtracting the horizontal component of the axial force from the actuator applied force at the top of the column. The resulting calculated base shears are shown in Fig. 9. The experimental results show that the seismically designed column made of RAC (Specimen No. 4) exhibited a similar cyclic behavior to that made of NAC (Specimen No. 2). However, the nonseismically designed column made of RAC (Specimen No. 3) possessed a lower strength than that made of NAC (Specimen No. 1). The experimental results presented in this section are compared to the results predicted by the numerical models.

NUMERICAL SIMULATION

Based on the four RC column specimens with nonseismic and seismic design (Fig. 3), and with natural concrete and recycled concrete, a pre-experimental numerical model for each corresponding RC column was created in *OpenSees* to predict the behavior of the RC column under the set of cyclic and axial loadings. Following the experiments, the numerical results were compared to the experimental results to evaluate the model accuracy.

To ensure a more accurate simulation, three-dimensional numerical models were developed. The column elements in the models (Fig. 10) were generated using force-based beam-column elements.[24] A rigid element (Element 7 in Fig. 10) was used to connect the column base and the center of the footing. The fiber sections consisting of concrete (676 fibers) and steel reinforcement were specified by considering uniaxial material objects of concrete-02, which is based on the Kent's model[25-27] (refer to Fig. 11), and hysteretic mate-

Table 3—Damage progression of experimentally tested columns

Specimen	Drift, %	Damage state	Photo
1	0.40	No significant cracking	Fig. 7 (1a)
	0.79	Cracks on north side; small cracks on east side	Fig. 7 (1b)
	1.58	Cracks around column base and on sides	Fig. 7 (1c)
	3.17	More cracks around column base	Fig. 7 (1d)
	4.75	More yielding cracks	Fig. 7 (1e)
	5.54	Spalling of concrete at column base	Fig. 7 (1f)
	7.12	Buckling of steel reinforcements	Fig. 7 (1g)
2	0.43	No significant cracking	NA
	0.87	Small cracks on south side	Fig. 7 (2a)
	1.77	Cracks on south side; small cracks on west side	Fig. 7 (2b)
	3.54	Cracks around column base and on sides	Fig. 7 (2c)
	5.37	Spalling of concrete at column base	Fig. 7 (2d)
	6.29	More cracks around column base; more yielding cracks	Fig. 7 (2e)
	7.20	Cover concrete failure around column base	Fig. 7 (2f)
	8.11	Buckling of steel reinforcements	Fig. 7 (2g)
3	0.45	Small cracks on north side	Fig. 7 (3a)
	0.90	Cracks on north side; small cracks on east side	Fig. 7 (3b)
	1.79	Cracks around column base and on sides	Fig. 7 (3c)
	3.58	More yielding cracks; concrete spalling around column base	Fig. 7 (3d)
	5.37	Cover concrete failure around column base	Fig. 7 (3e)
	6.27	Buckling of steel reinforcements	Fig. 7 (3f)
4	0.48	No significant cracking	Fig. 7 (4a)
	0.96	Small cracks on north side	Fig. 7 (4b)
	1.91	Cracks on south side; small cracks on west side	Fig. 7 (4c)
	3.82	Cracks around column base and sides	Fig. 7 (4d)
	5.73	More yielding cracks; concrete spalling around column base	Fig. 7 (4e)
	6.69	More cracks and cover concrete failure around column base	Fig. 7 (4f)
	7.64	Buckling of steel reinforcements	Fig. 7 (4g)

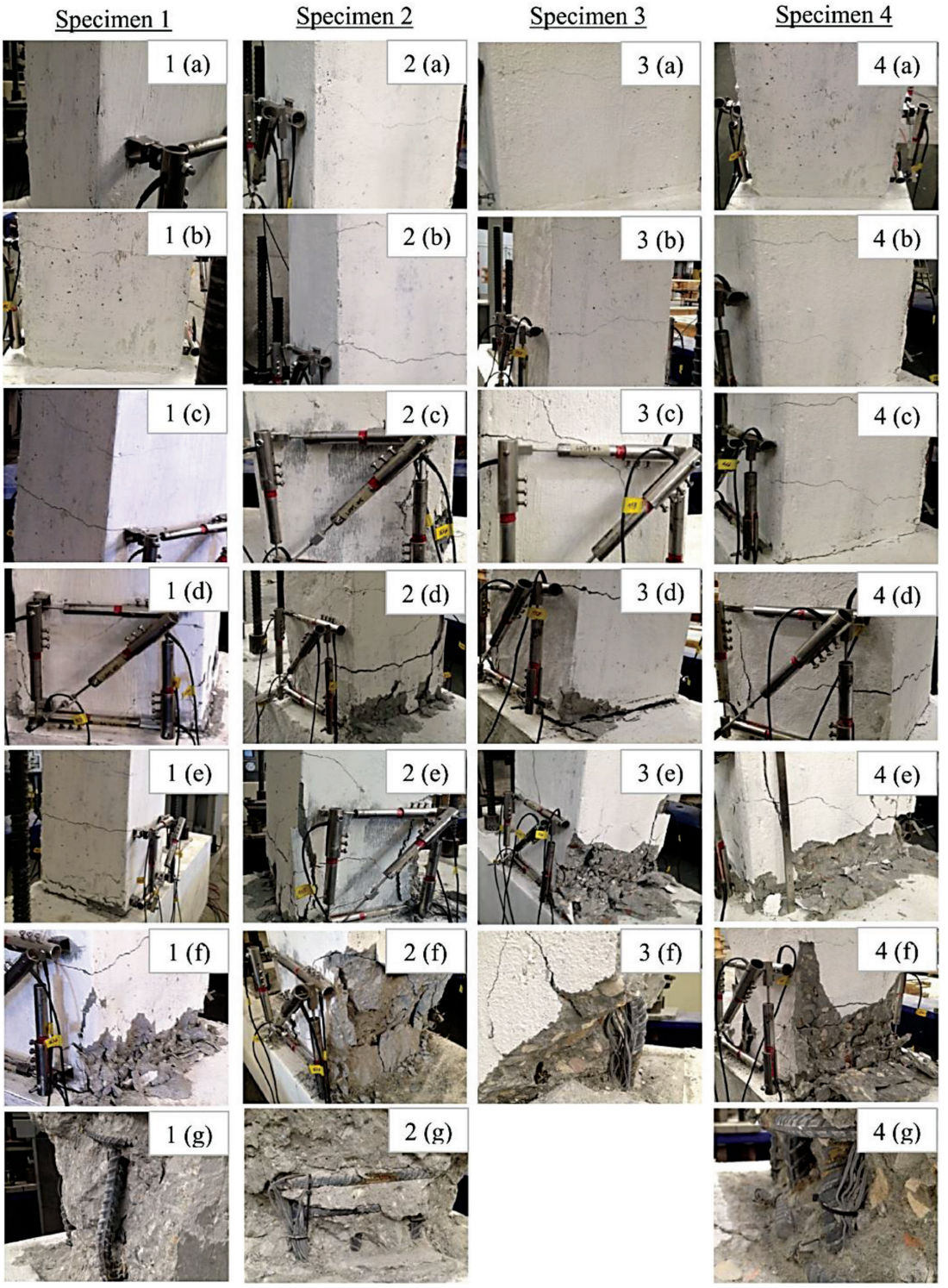

Fig. 7—Damage observed during experiments.

rial, respectively, in a nonlinear fiber-based finite element analytic platform of *OpenSees*. Different properties for the core concrete and the cover concrete were considered using the concrete models developed by Mander et al.[28] As depicted in Fig. 10, gravitational loads associated with the column self-weight were applied to the nodes in the column. In addition, the axial load corresponding to 10% of the axial capacity of the column was also included in the analysis. For the lateral loading simulation, a static cyclic analysis using a displacement control strategy was performed in the *OpenSees* models. The same cyclic displacements used in the experiments (Fig. 4) were also applied to the top of the columns.

Numerical results

To verify the feasibility of stress and strain parameters typically specified for concrete in the pre-experimental models, the accuracy of the models was assessed by comparing the experimental and numerical base shear versus lateral displacement results. In the pre-experimental models, the peak compressive stress (a parameter $fpc in

Fig. 11) of unconfined concrete was based on the results of the concrete test cylinders. Using the experimental modulus of elasticity of 3300 ksi (22,753 MPa) for NAC and 3820 ksi (26,338 MPa) for RAC, the concrete strain ($epsc0) at the maximum stress was determined based on Kent's model,[25,29] the concrete crushing stress ($fpcU) of 0.2 × $fpc was specified and the corresponding strain ($epsU) of 5 × $epsc was assumed. The tensile stress equal to 0.1 × $fpc, and the Lambda ratio equal to 0.1 were considered for all models.[30]

Following the numerical analysis, the base shear versus lateral displacement curves obtained from the pre-experimental models and the experiments (Fig. 12) were compared to evaluate the accuracy of strength using the following measure of relative error[31]

$$\text{relative error (\%)} = \frac{\sqrt{\sum_{i=1}^{n}(be_i - bn_i)^2}}{\sqrt{\sum_{i=1}^{n}(be_i)^2}} \quad (1)$$

in which *bn* and *be* are, respectively, the numerical and experimental base shear values, and *n* is the number of data points. The accuracy values (accuracy (%) = 100% – relative error (%)) of the numerical results for Specimens No. 1, 2, 3, and 4 were approximately 76%, 85%, 88%, and 86%, respectively. Generally, based on the summation of ($be_i - bn_i$), the numerical models overestimated the experimental results (refer to Fig. 12). From a design standpoint, Table 2 shows the strength comparison of specimens at 1% and 2% drift levels.

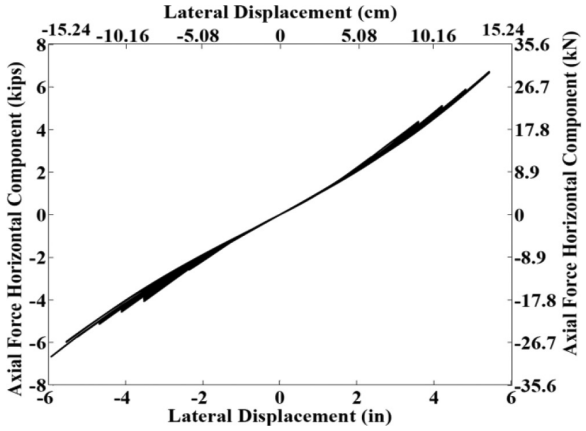

Fig. 8—Axial force horizontal component of Specimen No. 2.

DISCUSSION

In this study, both the concrete (NAC and RAC) and reinforcement detailing were selected as the test variables to find out the effect of both variables on the lateral response of the column specimens. A single source of RCA was meant to serve as a "low bar" for quality (that is, the RCA source

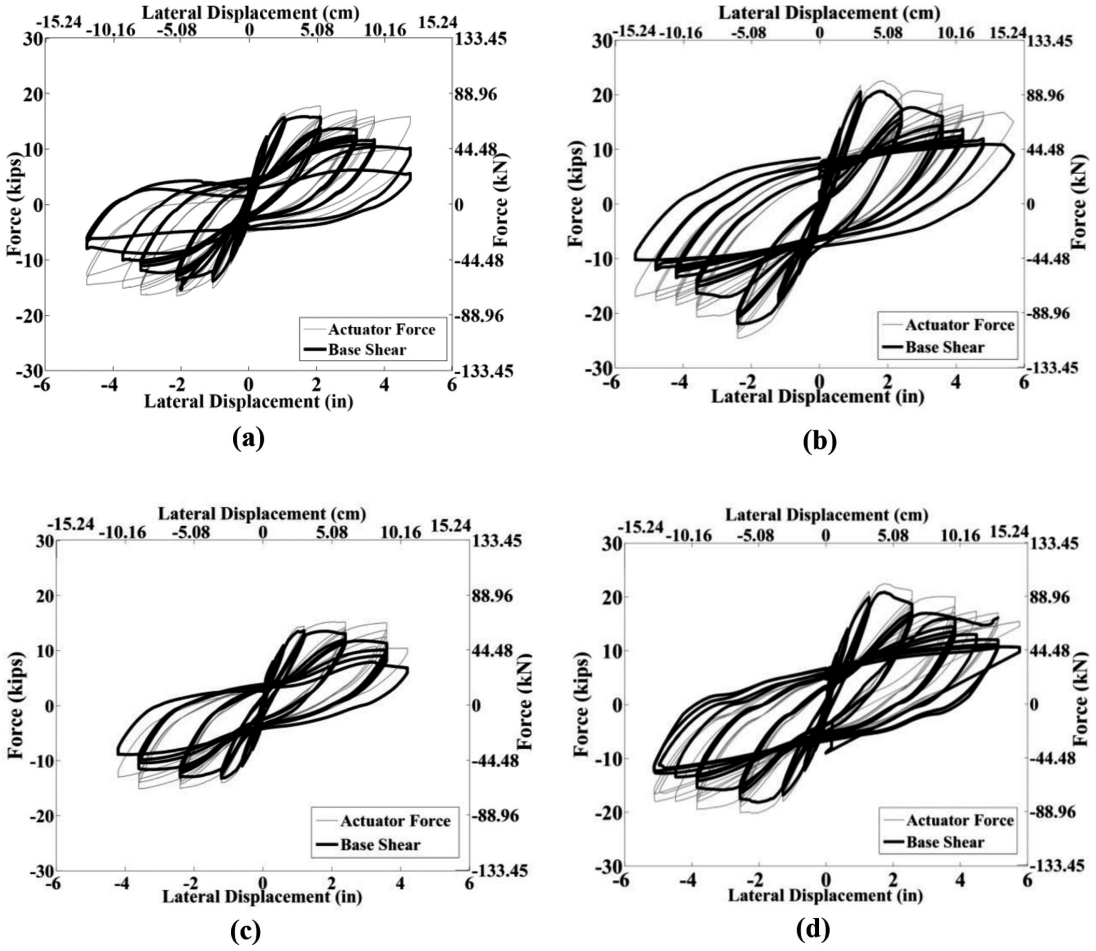

Fig. 9—Comparison of actuator force with base shear for Specimens: (a) No. 1; (b) No. 2; (c) No. 3; and (d) No. 4.

was selected because it was composed of relatively marginal construction and demolition debris). Overall, the nonseismically detailed RAC column (Specimen No. 3) showed the lowest resistance, and the seismically detailed RAC column (Specimen No. 4) was comparable to the seismically detailed column made with NAC (Specimen No. 2). Because the adequate seismic performance was observed in the seismically detailed columns (Specimens No. 2 and No. 4), the evaluation of the "low bar" RCA suggests that higher quality RCA should perform as well, if not better, in similarly detailed columns. Of course, additional testing may be warranted. However, it is believed that the selection of the marginal quality RCA does provide important new insight on the anticipated performance of RAC when appropriately designed.

Specimen No. 3 was the weakest among the four specimens and reached the failure of longitudinal reinforcement buckling at an earlier stage (Fig. 7(3f) and Table 3), so there is no Fig. 7(3g). Although the seismically designed column made of RAC appeared to have more damage than the column made of NAC at the stage shown in Fig. 7(4e) and 7(2e), the damage occurred in the unconfined concrete cover, not in the confined concrete core. This statement can be demonstrated in Fig. 7(4f), showing concrete cover spalling. It is interesting to note that sufficient lateral confinement can efficiently increase the strength and ductility of RAC.

In Fig. 9, Specimens No. 1 and No. 2 show a less stable phenomenon in the base shear versus displacement hysteresis loops. However, the lateral force on the top (that is, actuator force) versus displacement curves was stable. Figure 9 shows two different curves. One is the force measured from the load cell in the actuator (that is, the actuator force at the top of the specimens) and the other is the calculated base shear force (that is, the shear force at the column base, which is equal to the actuator force subtracted by the horizontal component of the axial force). Because the horizontal component of the axial force resulted in an effect of negative stiffness (self-recentering effect), the less stable (negative stiffness) situation could occur when the actuator force remained small, and the horizontal component of the axial force changed from large to small values. For example, in Specimen No. 1 in the range from –3 to –1 in. (76.2 to 25.4 mm), the actuator force increased from –1 to 0 kip (–4.45 to 0 kN); however, the horizontal component of the axial force increased from –4 to –1 kip (–17.79 to –4.45 kN). Hence, the calculated base shear force decreased from 3 to 1 kip (13.34 to 4.45 kN), resulting in negative stiffness.

The results from the numerical models with an average accuracy value of 84% were compared to the experimental findings. For the nonseismically designed specimens (Specimens No. 1 and No. 3), the accuracy percentage for the NAC column is 76%, which is lower than 88% for the RAC column. The lower accuracy percentage for the NAC column (Specimen No. 1) is because, in the post strength degradation range, there were more discrepancies on the forces between the pre-experimental numerical model and the experimental tests for Specimen No. 1 than for Specimen No. 3 (Fig. 12(a) and 12(c)). Thus, the pre-experimental numerical models cannot accurately predict the behavior of post strength degradation.

The finding can be verified by comparisons of curvatures around the column base (Fig. 13) and by comparisons of base

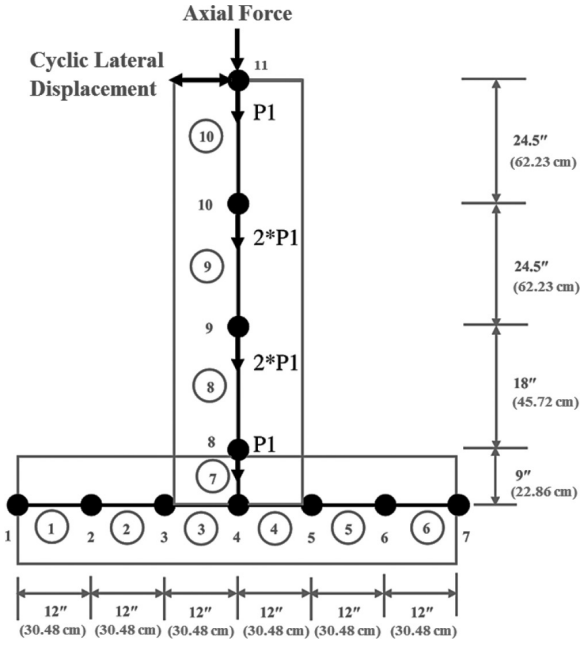

Fig. 10—Cantilever RC column model and assigned loads.

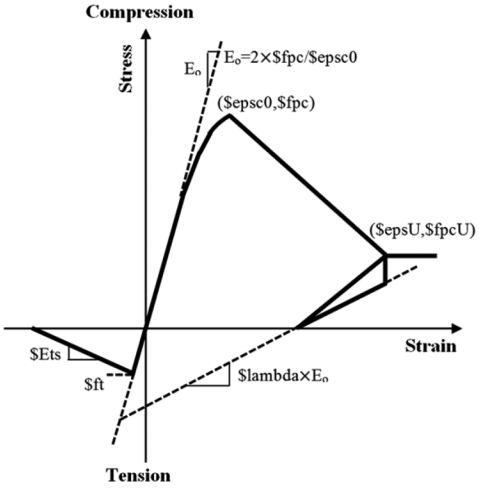

Fig. 11—Stress-strain curve for OpenSees Concrete-02.[11]

$fpc	compressive strength
$epsc0	strain at compressive strength
$fpcU	crushing strength
$epsU	strain at crushing strength
$lambda	ratio between unloading slope at $epscU and initial slope (E_o)
$ft	tensile strength
$Ets	tension softening stiffness

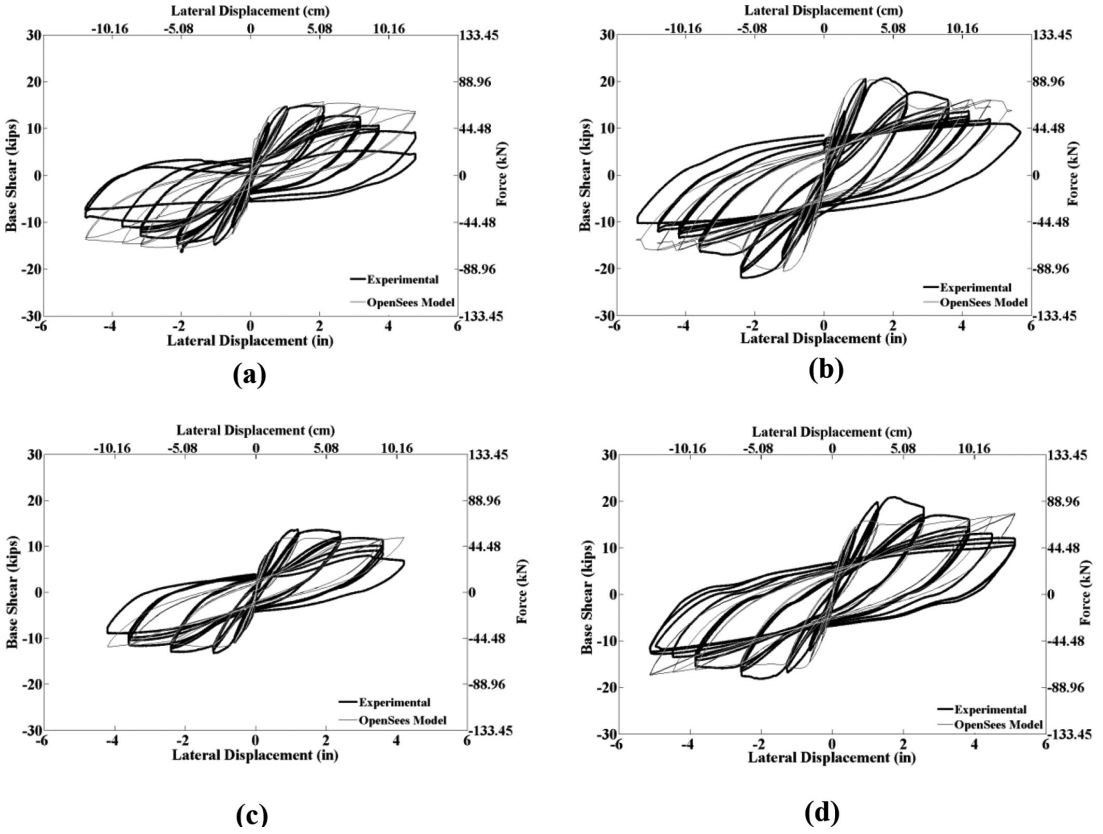

Fig. 12—Comparison of column base shears for Specimens: (a) No. 1; (b) No. 2; (c) No. 3; and (d) No. 4.

shear versus lateral displacement hysteresis response (Fig. 14). In the displacement range of 0 to 0.025 in. (0 to 0.6 mm), Specimen No.1 and Specimen No. 3 have quite similar curvatures. In the range of 0.025 to 0.06 in. (0.6 to 1.5 mm), Specimen No. 3 has higher curvatures at similar displacements than Specimen No. 1. However, column base curvatures of Specimens No. 2 and No. 4 are very similar. At large lateral displacements, the base shear for Specimen No. 3 is approximately 40% lower than the base shear for Specimen No. 1, indicating that Specimen No. 3 showed lower resistance; Specimen No. 3 experienced more damage. Notably, a significant decrease in the base shear for Specimen No. 3 at large lateral displacements is because of the lower strength of RAC in comparison with NAC and steel reinforcement yielding. Nevertheless, the results of base shear for Specimens No. 2 and No. 4 show very similar behavior. In particular, these columns maintained their capacity to continue carrying the base shear until the large lateral displacements. This is because the closely spaced ties effectively increased the concrete peak compressive stress and the corresponding strain as compared to completely unconfined NAC and RAC.

The results from the compressive tests of concrete cylinders without confinement show that the compressive strength of RAC was lower than that of NAC. The lower compressive strength significantly decreased the base shear at the large lateral displacements for the nonseismically designed column (Specimen No. 3). However, the results of base shear for seismically designed Specimens No. 2 and No. 4 showed very similar behavior. In particular, these columns maintained their capacity to continue carrying the base shear until the large lateral displacements. During the lateral cyclic tests, the axial loads applied in this study were constant based on the residual axial capacities of the column specimens. The residual axial load capacity of a reinforced concrete column can be estimated as 10% of the undamaged axial load capacity of the column.[10,23] This method of approximating the residual axial capacity is used where some information (for example, the effective friction coefficient and critical crack angle) is not available prior to experimental testing. For the investigation of the axial load capacity of a column, although the present study does not carry out the pure axial load tests without lateral loads and with gradually increasing axial loads until column failure, it can be expected that the unconfined concrete cover of an RAC column will crush and spall at early stages, but the confined concrete core provides a better strength and ductility than the unconfined portion. The realistic axial load capacity of RAC columns needs further investigation in the future.

Because the flexural capacity of Specimen No. 2 and No. 4 are comparable, further study can focus on evaluating the rotational capacity of the RAC columns. In this study, an initial investigation was conducted by installing linear variable displacement transducers (LVDTs) to the specimens during the tests. For Specimen No. 2 (Fig. 15(a)), when the moment decreased to 80 kip-ft (108.46 kN-m) from the yield moment, My = 139 kip-ft (188.46 kN-m), the rotation was 0.09 rad, and the column drift of Specimen No. 2 reached –5.5 in. (139.7 mm). The value of θ_u (that is, ultimate rotation) for Specimen No. 2 is set as 0.09 rad. However, for Specimen No. 4 (Fig. 15(b)), when the moment decreased to 80 kip-ft (108.46 kN-m), the rotation is 0.151 rad, and the column drift of Specimen No. 4 reached –5.5 in (139.7 mm). It is

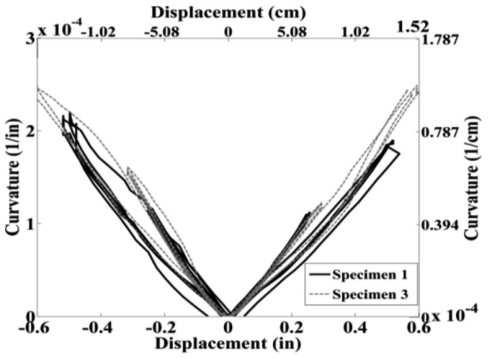

(a)

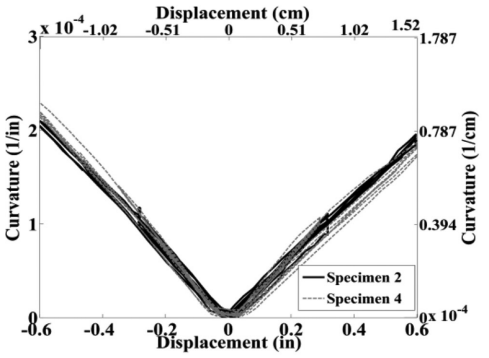

(b)

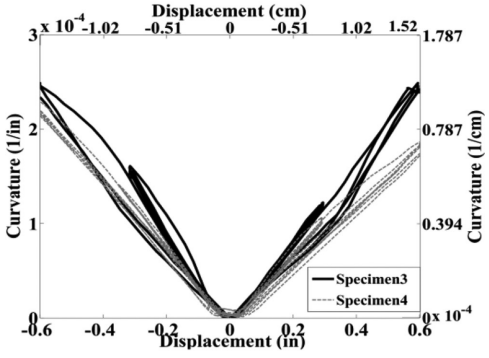

(c)

Fig. 13—Comparison of column base curvatures obtained from experiment: (a) Specimens No. 1 and 3; (b) Specimens No. 2 and 4; and (c) Specimens No. 3 and 4.

important to note that the moment capacity still remained approximately constant (80 kip-ft [108.46 kN-m]) even after the rotation 0.151 rad. To be conservative, the value of θ_u for No. 4 is set as 0.151 rad. In the aspect of yield rotation (θ_y), for Specimen No. 2, θ_y is approximately 0.0040, whereas for Specimen No. 4, θ_y is approximately 0.0035. The rotation capacity ($C_r = (\theta_u - \theta_y)/\theta_y = \theta_u/\theta_y - 1$) is calculated as 21.50 and 41.86 for Specimens No. 2 and No. 4, respectively. The computed values of C_r indicate that Specimen No. 4 has a higher rotation capacity than Specimen No. 2.

CONCLUSIONS

In this research, cyclic quasi-static testing of four RC columns containing natural aggregate concrete (NAC) and

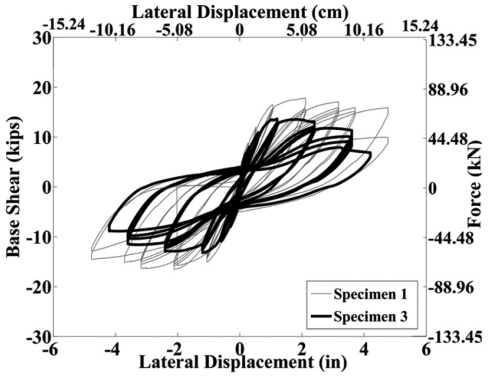

(a)

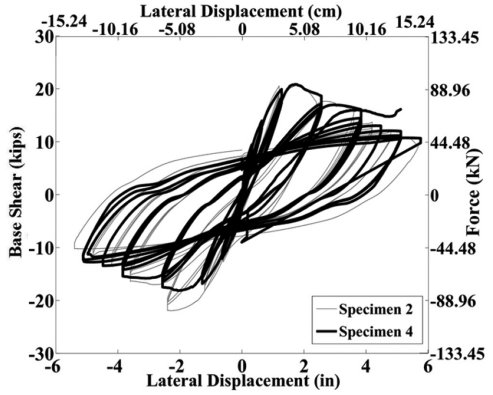

(b)

Fig. 14—Comparison of column base shear obtained from experiment: (a) Specimens No. 1 and 3; and (b) Specimens No. 2 and 4.

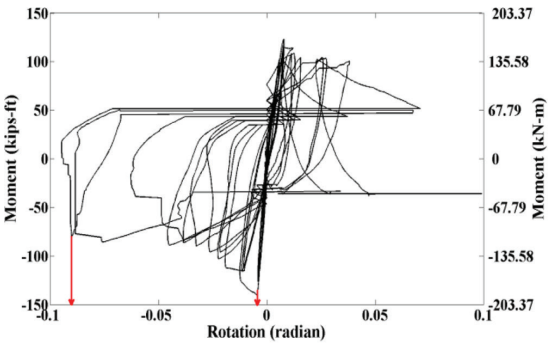

(a)

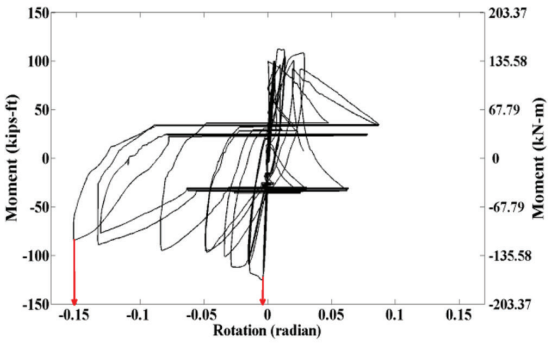

(b)

Fig. 15—Moment-rotation relationship for Specimens: (a) No. 2; and (b) No. 4.

recycled aggregate concrete (RAC) was performed. For each type of aggregate, a nonseismically and seismically detailed column was tested. The compressive strengths for natural and recycled concrete were approximately 4500 and 2800 psi (31.0 and 19.3 MPa), respectively. The experimental results from the column tests show that the nonseismically designed RC columns containing RAC exhibited lower strength than the nonseismically designed columns made with NAC. However, the seismically detailed column containing RAC exhibited a similar cyclic behavior to the seismically designed column made with NAC. Both seismically designed columns with NAC and RAC exhibited similar strength and ductile behavior, and maintained their flexural and shear capacities at large lateral displacement ratios up to 4.0%.

The *OpenSees* models were able to reproduce the cyclic behaviors of the tested specimens in conformance to the experimental results, with the accuracy values of 76%, 85%, 88%, and 86%, respectively, for Specimens No. 1, 2, 3, and 4. On the basis of the results obtained through the experiments and numerical simulations, it is concluded that in the seismically designed columns, NAC can be replaced by RAC without significant changes in the cyclic behavior. Moreover, it was determined that the use of proper seismic detailing, particularly adequately spaced transverse reinforcement, is critical in ensuring adequate behavior for columns with RAC.

AUTHOR BIOS

Farahnaz Soleimani *is a PhD Candidate at the Georgia Institute of Technology (Georgia Tech), Atlanta, GA. She received her bachelor's degree in civil engineering from Sharif University of Technology, Tehran, Iran, and her master's degree in structural engineering from Tufts University, Medford, MA. Her research interests include finite element analysis and damage identification, structural reliability, fragility analysis, and performance of advanced materials for structures.*

Mitchell McKay *is a Structural Engineer at Enercon Services, Inc., Atlanta, GA. He received his MS and BS in civil and environmental engineering from Georgia Tech. His research interests include the use and recyclability of construction materials in the Caribbean region.*

C. S. Walter Yang *is a Research Engineer and Lecturer at Georgia Tech, where he received his doctoral degree and two master's degrees in civil and mechanical engineering. His research interests include seismic design and behavior of buildings and bridges, dynamic structural tests, smart structures, and seismic probabilistic assessment.*

Kimberly E. Kurtis, *FACI, is a Professor in the School of Civil and Environmental Engineering at Georgia Tech. She is a past Chair of ACI Committee 236, Material Science of Concrete, and is a member the ACI Technical Activities Committee (TAC).*

Reginald DesRoches *is the Karen and John Huff School Chair and Professor of Civil and Environmental Engineering at Georgia Tech. His research interests include seismic design of buildings, critical infrastructure, and seismic risk assessment of lifeline systems.*

Lawrence F. Kahn, *FACI, is a Professor in the School of Civil and Environmental Engineering at Georgia Tech. He is a past Chair and current member of ACI Committee 562, Evaluation, Repair, and Rehabilitation of Concrete Buildings, and ACI Committees 364, Rehabilitation; 546, Repair of Concrete; and the ACI Technical Activities Committee.*

ACKNOWLEDGMENTS

The authors and the Caribbean Hazard Assessment Mitigation and Preparedness (CHAMP) Initiative would like to thank the Speedwell Foundation for their generous support. The authors would also like to thank A. Jayapalan for his collaboration and assistance.

REFERENCES

1. Government of Haiti, "Action Plan for National Recovery and Development of Haiti," Government of the Republic of Haiti, Mar. 2010, pp. 6-8.

2. Miyamoto, H. K.; Gilani, A. S. J.; and Wong, K., "Massive Damage Assessment Program and Repair and Reconstruction Strategy in the Aftermath of the 2010 Haiti Earthquake," *Earthquake Spectra*, V. 27, 2011, pp. S219-S237. doi: 10.1193/1.3631293

3. Mwasha, A., and Lalla, J. R. F., "Analyzing the Strength Parameters of Concrete Manufactured Using Natural and Recycled Guanapo Aggregates," *The West Indian Journal of Engineering*, V. 34, No. 1/2, 2011, pp. 44-51.

4. Lalla, J. R. F., and Mwasha, A., "Comparing the Compressive Strengths of Guanapo Recycled Aggregate Concrete with That of Its Waste Material," *10th LACCEI Latin American and Caribbean Conference*, Panama City, Panama, July 23-27, 2012, pp. 1-9.

5. Rahal, K., "Mechanical Properties of Concrete with Recycled Coarse Aggregate," *Building and Environment*, V. 42, No. 1, 2007, pp. 407-415. doi: 10.1016/j.buildenv.2005.07.033

6. Corinaldesi, V.; Letelier, V.; and Moriconi, G., "Behaviour of Beam-Column Joints Made of Recycled-Aggregate Concrete under Cyclic Loading," *Construction and Building Materials*, V. 25, No. 4, 2011, pp. 1877-1882. doi: 10.1016/j.conbuildmat.2010.11.072

7. Elwood, K. J., and Moehle, J. P., "Shake Table Tests and Analytical Studies on the Gravity Load Collapse of Reinforced Concrete Frames," *Pacific Earthquake Engineering Research Center, Report Series*, University of California Berkeley, Berkeley, CA, Nov. 2003, pp. 97-227.

8. Tasai, A., "Residual Axial Capacity of Reinforced Concrete Columns during Shear Deterioration," *2nd U.S.-Japan Workshop on Performance-Based Earthquake Engineering Methodology for Reinforced Concrete Building Structures*, Sapporo, Japan, 2000, pp. 257-267.

9. Minowa, C.; Ogawa, N.; Hayashida, T.; Kogoma, I.; and Okada, T., "Dynamic and Static Collapse Tests of Reinforced-Concrete Columns," *Nuclear Engineering and Design*, V. 156, No. 1-2, 1995, pp. 269-276. doi: 10.1016/0029-5493(94)00968-5

10. Flores, L. M., "Performance of Existing Reinforced Concrete Columns under Bidirectional Shear & Axial Loading," *Research Report*, University of California, San Diego, San Diego, CA, 2004, pp. 14-38.

11. OpenSees, "Open System for Earthquake Engineering Simulation," *Pacific Earthquake Engineering Research Center*, University of California Berkeley, Berkeley, CA, http://opensees.berkeley.edu/ (last accessed Oct. 2013)

12. IBC 2000, "International Building Code," Washington, DC, 2000, pp. 146-497.

13. AASHTO M 43, "Standard Specification for Sizes of Aggregate for Road and Bridge Construction," American Association of State Highway and Transportation Officials, Washington, DC, 2009.

14. ASTM C39/C39M-10, "Standard Test Method for Compressive Strength of Cylindrical Concrete Specimens," ASTM International, West Conshohocken, PA, 2010, 7 pp.

15. ASTM C469-94, "Standard Test Method for Static Modulus of Elasticity and Poisson's Ratio of Concrete in Compression," ASTM International, West Conshohocken, PA, 1994.

16. ACI Committee 211, "Standard Practice for Selecting Proportions for Normal, Heavyweight, and Mass Concrete (ACI 211.1-91)," American Concrete Institute, Farmington Hills, MI, 1991, 38 pp.

17. DesRoches, R. R.; Kurtis, K. E.; and Gresham, J. J., "Breaking the Reconstruction Logjam: Haiti Urged to Recycled Concrete Rubble," *Bulletin of the American Ceramic Society*, V. 90, No. 1, Jan./Feb. 2011, pp. 20-26.

18. Ravindrarajah, R. S., and Tam, C. T., "Properties of Concrete Made with Crushed Concrete as Coarse Aggregate," *Magazine of Concrete Research*, V. 37, No. 130, 1985, pp. 29-38. doi: 10.1680/macr.1985.37.130.29

19. Frondistou-Yannas, S., "Waste Concrete as Aggregate for New Concrete," *ACI Journal Proceedings*, V. 74, No. 8, Aug. 1977, pp. 373-376.

20. Lopez, M.; Kahn, L. F.; and Kurtis, K. E., "Characterization of Elastic and Time-Dependent Deformations in High Performance Lightweight Concrete by Image Analysis," *Cement and Concrete Research*, V. 39, No. 7, 2009, pp. 610-619. doi: 10.1016/j.cemconres.2009.03.015

21. Hashin, Z., and Monteiro, P. J. M., "An Inverse Method to Determine the Elastic Properties of the Interphase between the Aggregate and the Cement Paste," *Cement and Concrete Research*, V. 32, No. 8, 2002, pp. 1291-1300. doi: 10.1016/S0008-8846(02)00792-5

22. Li, C. Q., and Zheng, J. J., "Closed-Form Solution for Predicting Elastic Modulus of Concrete," *ACI Materials Journal*, V. 104, No. 5, Sept.-Oct. 2007, pp. 539-546.

23. Terzic, V.; Mackie, K.; and Stojadinovic, B., "Experimental Evaluation of the Residual Axial Load Capacity of Circular Bridge Columns," *14th World Conference on Earthquake Engineering*, Beijing, China, 2008, pp. 1-8.

24. Mazzoni, S.; McKenna, F.; Scott, M. H.; Fenves, G. L. et al., "Open System for Earthquake Engineering Simulation User Command-Language Manual," Pacific Earthquake Engineering Research Center, University of California Berkeley, Berkeley, CA, V. 1.7.3., 2006, pp. 213-243, http://opensees.berkeley.edu/OpenSees/manuals/usermanual/OpenSeesCommandLanguageManualJune2006.pdf.

25. Kent, D., "Inelastic Behavior of Reinforced Concrete Members with Cyclic Loading," doctoral thesis, University of Canterbury, Christchurch, New Zealand, 1969, pp. 108-125.

26. Scott, B. D.; Park, R.; and Priestley, M. J. N., "Stress-Strain Behavior of Concrete Confined by Overlapping Hoops at Low and High Strain Rates," *ACI Journal Proceedings*, V. 79, No. 2, Mar.-Apr. 1982, pp. 13-27.

27. Song, W.; Dyke, S.; Harmon, T.; and So, M., "Nonlinear Model Updating in Concrete Structures Based on Ambient Response Data," *Proceedings of 27th International Modal Analysis Conference*, Society for Experimental Mechanics (SEM), Bethel, CT, 2009, pp. 99-124.

28. Mander, J. B.; Priestley, M. J. N.; and Park, R., "Theoretical Stress-Strain Model for Confined Concrete," *Journal of Structural Engineering*, ASCE, V. 114, No. 8, 1988, pp. 1804-1826. doi: 10.1061/(ASCE)0733-9445(1988)114:8(1804)

29. Roy, H. E. H., and Sozen, M. A., "Ductility of Concrete," *Proceedings of the Joint ACI-ASCE International Symposium on Flexural Mechanics of Reinforced Concrete*, Miami, FL, 1964, pp. 213-235.

30. Arioglu, N.; Girgin, Z. C.; and Arioglu, E., "Evaluation of Ratio between Splitting Tensile Strength and Compressive Strength for Concretes up to 120 MPa and Its Application in Strength Criterion," *ACI Materials Journal*, V. 103, No. 1, Jan.-Feb. 2006, pp. 18-24.

31. Golub, G. H., and Van Loan, C. F., *Matrix Computations*, third edition, The Johns Hopkins University Press, Baltimore, MD, 1996, pp. 52-53.